Purdue University
Purdue e-Pubs

International Refrigeration and Air Conditioning Conference

School of Mechanical Engineering

2016

Local Heat Transfer Characteristics of the R1234ze(E) Two Phase Flow Inside a Plate Heat Exchanger

Keishi Kariya
Saga university, Saga, Japan, kariya@me.saga-u.ac.jp

Mohammad Sultan Mahmud
Saga university, Saga, Japan, sultan_kuet01@hotmail.com

Akitoshi Kawazoe
Saga university, Saga, Japan, 14575009@edu.cc.saga-u.ac.jp

Akio Miyara
Saga university, Saga, Japan, miyara@me.saga-u.ac.jp

Local heat transfer characteristics of the R1234ze(E) two phase flow inside a plate heat exchanger

Keishi KARIYA[1]*, Mohammad Sultan MAHMUD[2], Akitoshi KAWAZOE[2] and Akio MIYARA[1]

[1] Department of Mechanical Engineering, Saga University, 1 Honjo-machi, Saga, 840-8502, Japan
Tel: +81-952-28-8608, E-mail: kariya@me.saga-u.ac.jp

[2] Graduate School of Science and Engineering, Saga University, 1 Honjo-machi, Saga, 840-8502, Japan

ABSTRACT

In the present study, condensation and evaporation local heat transfer coefficients of the R1234ze(E) inside a brazed plate heat exchanger were investigated by using a test section which is combined with two grooved stainless steel plates. In the test section, wall temperature distribution was measured. The test section consists of eight plates; two of them were processed herringbone for refrigerant flow channel other two flat plates are set for cooling plate for refrigerant, and another consist on cooling water flow channel. In order to measure local heat transfer and temperature distribution, five thermocouples were set at not only flow direction but also in the right and left sides of plates. Local heat transfer coefficient and temperature distribution were calculated from wall temperature and local heat flux with downward and upward flow condition.

1. INTRODUCTION

In the technical field of refrigeration and air-conditioning, plate heat exchangers are getting attention due to their compactness and high thermal efficiency. Although these were mainly designed for liquid heat exchanger, its application was extended to two phase heat exchangers such as condensers and evaporators. Condensation and evaporation heat transfer coefficients in plate heat exchangers have been studied by many researchers. Most of the existing literatures, however, discussed mainly overall heat transfer characteristics (Longo et al., 2010, Yan et al., 1999). Local heat transfer behavior has not been clarified sufficiently. Because of the effects on global warming by the refrigerants used in the present heat pump/refrigeration systems, new synthetic refrigerants, hydrofluoroolefins (HFOs), which have low global warming potential (GWP) are recently getting attention as next generation refrigerants (Miyara et al., 2012). However, many of HFOs has low flammability and expensive. Therefore, systems in which small amount of refrigerant is charged are required. From the view point of refrigerant charge reduction, plate heat exchangers are getting attention. When the plate heat exchangers are used as evaporator and/or condenser, maldistribution of refrigerant flow occurs in channels between the plates and headers to distribute it to the channels. This maldistribution deteriorates the heat exchanger performance. And local heat transfer coefficient may vary at flow direction and width direction in plate heat exchangers. It is important to investigate flow characteristics for understanding the heat transfer characteristic and for enhancing the heat transfer. Only a few reports about experimental flow observation of two phase flow in the plate heat exchanger. Asano et al. (2007) carried out the visualization of gas-liquid two phase flow by neutron radiography. Void fraction distributions in the plate heat exchanger were also measured. Arima et al. (2012) carried out flow observations and void fraction measurements on evaporation of ammonia flowing in parallel plates instead of an actual channel of plate heat exchangers. Experiments on condensation and evaporation heat transfer of low GWP refrigerants, R1234yf and R1234ze(E), in a plate heat exchanger have been carried out by Longo et al. (2012, 2013, 2014). Heat transfer coefficients and pressure drops in the condensation and evaporation of R1234ze(E) and R1234yf were measured and effects of saturation temperature, refrigerant mass flux and vapour super-heating are discussed. The data have been obtained from overall heat transfer performance and there is no sufficient discussion about local heat transfer characteristics. The local heat transfer coefficient varies not only flow direction but also width direction by gas-liquid distribution. In order to further understand the heat transfer characteristics, information about the local heat transfer is necessary. But measurements of local wall temperatures and heat fluxes are difficult because of the complicated structure. In the present study, a specially designed test section has been constructed for the measurement of local heat transfer coefficient. Experiments on condensation and evaporation heat transfer of a low GWP refrigerant, R1234ze(E) were carried out and local heat transfer characteristics were discussed.

2. EXPERIMENTAL APPARATUS AND THE DATA REDUCTION METHOD

2.1 Flow Loop of Refrigerant

Figure 1 indicates experimental flow loop of refrigerant. It mainly consists of magnet pump, pre-heater, test section and after condenser. After the refrigerant flows from magnet pump, mass flow rate is measured by coriolis flow meter. Then the refrigerant is heated by the pre-heater to set a designated enthalpy condition at the inlet of test section. After the refrigerant flows out through the test section, it is cooled by the after condenser to keep a certain subcooling. And the subcooled liquid comes back to the magnet pump. Mixing chambers are installed at inlet of the pre-heater and inlet and outlet of the test section to obtain the bulk enthalpy from measured refrigerant pressure and temperature at the mixing chamber. The refrigerant is heated or cooled by water of which temperature is controlled by thermostatic bath. The flow rate of refrigerant is controlled by the flow control valve and the rotation speed of magnet pump.

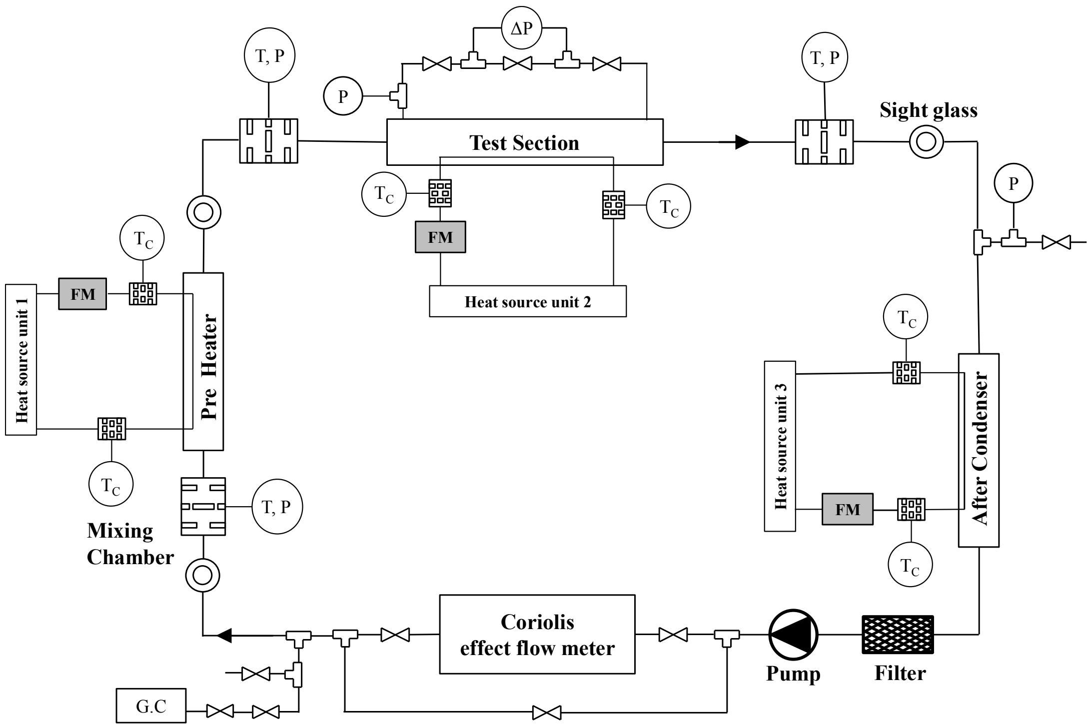

Figure 1: Schematic diagram of refrigerant flow loop

2.2 Test Section

For the measurement of local heat transfer characteristics of plate heat exchanger, a specially designed test section has been produced same as our previous study (Kawazoe et. al, 2015). Figure2 shows the schematic of test section and the installed points of thermocouples with the photograph. Chevron shape grooved are dug over a stainless steel plate of which length, width and thickness are 186mm, 84mm and 5mm respectively. The pitch and depth are 5.6mm and 1.5mm, respectively. A channel of the plate heat exchanger where the refrigerant flows is constructed by facing two grooved plats. Next of the grooved plates, flat plates are set to measure heat flux. Plates for the water channel are set outside of the flat plates. Whole of the test section is constructed with eight different kinds of plates which are brazed each other. The chevron directions of each plates which make a refrigerant flow channel are reversely assembled so that heat transfer enhance. The flat plates with 10mm in thickness have holes of 1.6mm in diameter on both sides where wire T-type thermocouples are installed and temperatures are measured. Positions of the temperature measurement are set at 23.2, 45.6, 68, 90.4 and 112.8mm from inlet of refrigerant channel.

Temperatures of local heat transfer surface at refrigerant and water sides are estimated from the measured temperature as explained later. The temperatures are also used to calculate the heat flux and heat transfer coefficient. The water channels consist of flat plates and the channel height is 5mm. Water flows into the channels from both sides of the test section, front and back. In should be noted, surface which have the inlet/outlet ports of refrigerant is called as inlet side and another side is call as opposite side. In addition, the center region is set for temperature measurement between the inlet and the opposite side as shown in the figure. The geometrical characteristics of the test section are listed in Table 1.

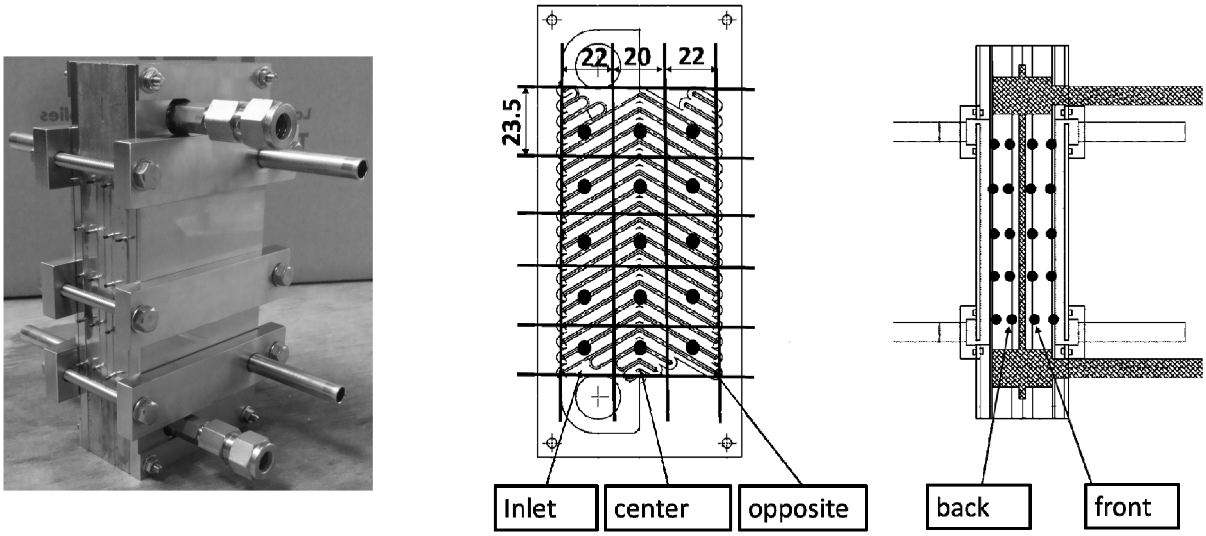

Figure 2: Photograph and Schematic of test section and place of temperature measurement

Table 1: Geometrical characteristics of the test section

Fluid flow plate length (mm)	117.5
Plate width (mm)	64
Area of the plate (m^2)	0.75
Corrugation type	Chevron
Angle of the corrugation (°)	60
Corrugation pitch (mm)	5.6
Number of plates	8
Number of channels on refrigerant side	1
Number of channels on water side	2

2.3 Data Reduction Method

By assuming the steady sate one-dimensional heat conduction, the local heat flux q_x in test section is calculated from the temperatures measured at both sides of 10mm thick flat plates.

$$q_x = \frac{T_{w,ref} - T_{w,water}}{l_1} \lambda \tag{1}$$

Where $T_{w,ref,}$ is temperature of measurement place of refrigerant side, $T_{w,\,water}$ is temperature of measurement place of water side, l_1 is distance between each K-type thermocouples. λ is the thermal conductivity of the stainless steel plate. Wall surface temperature of refrigerant side is calculated with the following equation where the linear temperature distribution is assumed and the temperature is extrapolated to the representative of surface of refrigerant side. l_2 in the equation is the distance between the K-type thermocouple and the average surface of the refrigerant side.

$$T_{wall,x} = T_{w.ref} \pm \frac{q_x l_2}{\lambda} \tag{2}$$

The plus-minus sign means the plus for condensation experiment, and the minus for evaporation experiment.
The local heat transfer coefficient h_x is defined with the following equation.

$$h_x = \frac{q_x}{T_{wall,x} - T_{sat}} \tag{3}$$

Where, T_{sat} is the saturation temperature of refrigerant which is calculated from measured pressure. q_x and $T_{wall,x}$ are calculated with Eq.(1) and (2), respectively.
The local thermodynamic equivalent quality x in the plate channel is calculated by following equation.

$$x = \frac{i_x - i_l}{L} \tag{4}$$

And the wetness is given as (1-x).Where i_x is the local specific enthalpy of the refrigerant, i_l is the specific enthalpy of saturated liquid. The local specific enthalpy can be calculated from the heat balance equation at the specific position, as explained in the following method.
First, specific enthalpy at inlet of pre-heater $i_{pre,in}$ is calculated by REFPROP. And, the specific enthalpy at the test section inlet is calculated from the mass flow rate $\dot{m}$ and the heat transfer rate in the pre-heater Q_{pre}. Then specific enthalpy of inlet at test section i_{in} is calculated by follow equation.

$$i_{in} = i_{pre,in} + \frac{Q_{pre}}{\dot{m}} \tag{5}$$

Finally, the local specific enthalpy in the test section is calculated from mass flow rate $\dot{m}$ and the heat transfer rate from the inlet to a certain point which is obtained by integrating the heat flux, as expressed with the following equation.

$$i_x = i_{in} + \frac{1}{\dot{m}} \int_0^{A_x} q dA \tag{6}$$

3. RESULT AND DISCUSSION

3.1 Experimental Condition

Table2 indicates experimental conditions of the present study. Refrigerant tested is R1234ze(E) which is one of the promising candidates of the next generation refrigerants and has the low GWP < 1 (5th IPCC). Flow direction of the refrigerant is the downward for condensation test and the upward for evaporation test. Saturated temperature are 35-40 °C and 5-10 °C for condensation and evaporation tests, respectively. Mass flux conditions are 10 and 20 kg/(m^2·s) in both experiments. In the case of condensation experiment, temperature of cooling water (heat source at the test section) is controlled in order that the refrigerant flows into the test section as nearly saturated vapor state and flows out as nearly saturated liquid. In the case of evaporation experiment, nearly saturated liquid enters and nearly saturated vapor exits.

Table 2: Experimental conditions

	Flow direction	T_{sat}[°C]	G[$kgm^{-2}s^{-1}$]	x_{in}[-]	x_{out}[-]
Condensation	downward	35-40	10, 20	0.9-1.0	0.0-0.1
Evaporation	upward	5-10	10, 20	0.0-0.1	0.9-1.0

3.2 Results of Condensation

Figure 3 shows wall temperature distributions in the test section of a condensation experiment with G=10 [kg/m^{2}s] and q=20 [kW/m^2]. The temperatures decrease gradually toward the distance along downstream which is the direction of condensation progress. The temperature difference between the front side and back side is small. On the other hand, there are notable temperature differences between the front inlet part and other parts of the plate surface. And the temperature difference indicates the peak at the second temperature measuring point (z = 35.25 mm). The similar tendency is obtained in our previous study (Kawazoe et. al, 2015). From this result, it is inferred that maldistribution of condensate flow occurs in the channel of plate heat exchangers.

Figure 4 shows the local heat transfer coefficient versus wetness at the same condition in figure3. The values of wetness are average values of horizontal cross section which are calculated from heat balance of the measured heat flux as explained in previous section. As wetness increases, heat transfer coefficient decreases as a general behaviour of condensation. The thickness of liquid film increases with increase of wetness and it generally prevents heat transfer. In the comparison of distribution of heat transfer coefficient at the plate cross section, the value of both front and back inlet side is lower than the others. It is also found that value of the heat transfer coefficient at the front inlet side is lower than that of the back side. In our observation of air-water two phase flow (Eshima et al., 2013), liquid flow mainly in the center and both edge of the plate, and differences between inlet and opposite are hardly observed. Because the reason of the difference of condensation heat transfer coefficient cannot be explained from the observation, further investigation is required.

The local condensation heat transfer coefficient of vertical plate can be calculated by the Nusselt's liquid-film theory.

$$h_{x,Nusselt} = 0.707\left[\frac{\lambda_L^3 g \rho_L^2 L}{\mu_L l_3 \left(T_{sat} - T_{wall,x}\right)}\right]^{0.25} \tag{7}$$

Where g is gravitational acceleration, ρ_L is liquid density, L is latent heat, μ_L is liquid viscosity, l_3 is length of heat transfer surface, $T_{wall,x}$ is average of wall temperature in horizontal direction. In the low wetness region, experimental values are about two times higher than those calculated by Eq.(7). And the experimental value approaches to the Nusselt's equation with increase of wetness and at last the measurement indicate lower value than Nusselt's equation.

Figure 5 shows wall temperature distributions in the test section of a condensation experiment with G=20 [kg/m^{2}s] and q=20 [kW/m^2]. As shown in the figure, similar tendency of temperature distribution to the condition of G=10 [kg/m^{2}s] are shown. On the other hand, as seen in the figure 6, the characteristics of heat transfer coefficient is different. The difference of value of heat transfer coefficient is larger than the case of G=10 [kg/m^{2}s] especially at the second measurement point (at wetness of 0.4). Generally the maldistribution in the cross section direction of the plate surface seems to be lower with increasing mass flux. The characteristics of local heat transfer inside plate are affected by the flow characteristics. To clarify flow characteristics is required in the future work.

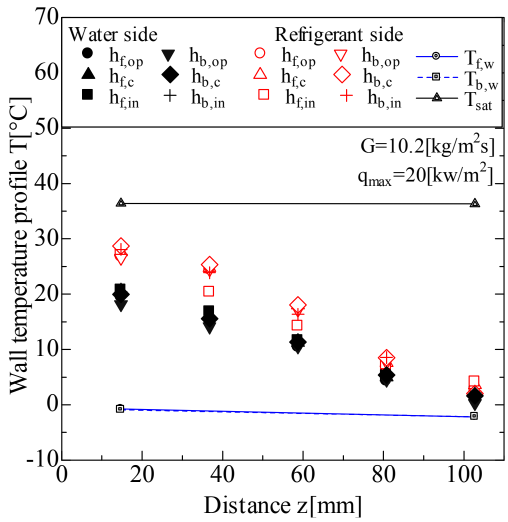

Figure 3: Temperature distribution of wall in condensation experiment (G = 10 kg/m^{2}s)

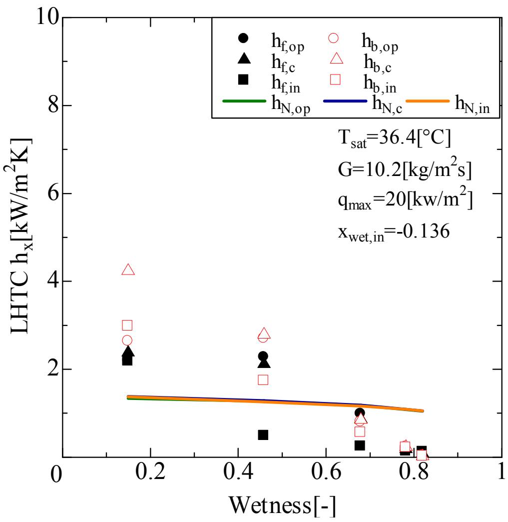

Figure 4: Local heat transfer coefficient of condensation experiment (G = 10 kg/m^{2}s)

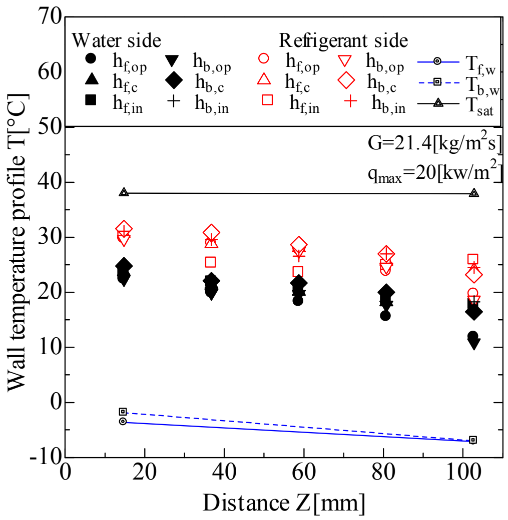

Figure 5: Temperature distribution of wall in condensation experiment (G = 20 kg/m^{2}s)

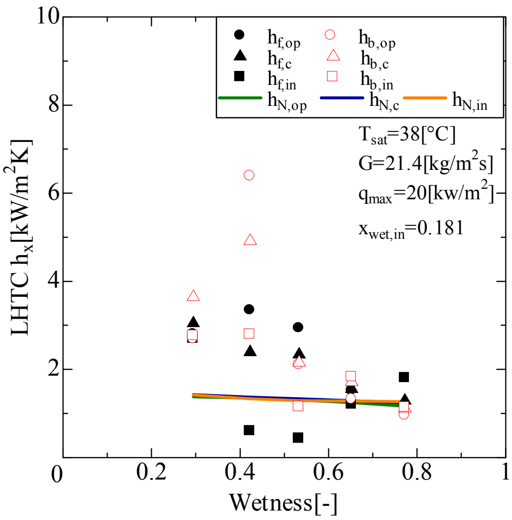

Figure 6: Local heat transfer coefficient of condensation experiment (G = 20 kg/m^{2}s)

3.3 Result of Evaporation

Figure 7 shows wall temperature distributions in test section of an evaporation experiment with G=10 [kg/m^{2}s] and q=20 [kW/m^2]. In the evaporation experiments, refrigerant flows upward and heating water flows downward countercurrently. The wall temperature increased with increase of the distance with is the direction of evaporation progress. Like the experiment of condensation, temperature differences between the front and back is small. The difference between inlet, center and opposite side is small at all measurement points. This fact are suggested that refrigerant of the evaporation (upward flow) flows uniformly compared with the case of the condensation (downward flow). However, refrigerant temperatures at *z*=58.75 mm approach to water (heat source) temperature due to dryout occurred at *z*=58.75 mm therefore the maldistribution still occurs.

Figure 8 shows local heat transfer coefficient versus quality at the same condition in figure 7. At the first temperature measurement point, the value of heat transfer coefficient of back side are higher than the value of the

front side and the values becomes similar with the flow toward the downstream. It is also found that the value of heat transfer coefficient of the inlet side are higher than that of the opposite side and the value at the center of the plate is similar to the inlet side. This result is caused by maldistribution i.e. much liquid flows at the inlet side.
Figure 9 shows wall temperature distributions in test section of an evaporation experiment with G=20 [kg/m^{2}s] and q=28 [kW/m^2]. As shown in the figure, wall temperature increase with increasing the distance and the temperature of opposite sides at z=112 mm abruptly increase due to occurrence of dryout.
Figure 10 shows wall temperature distributions in the test section of an evaporation experiment with G=20 [kg/m^{2}s] and q=28 [kW/m^2]. It is found that the value of heat transfer coefficient at the front side are lower than back side especially at the first temperature measuring point. After the first point, the value both the front and back side approach and indicate similar value but the value of the front inlet side keep lower value.

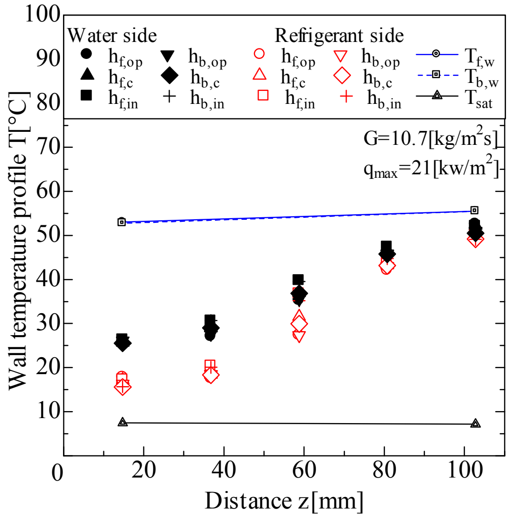

Figure 7: Temperature distribution of wall in evaporation experiment (G = 10 kg/m^{2}s)

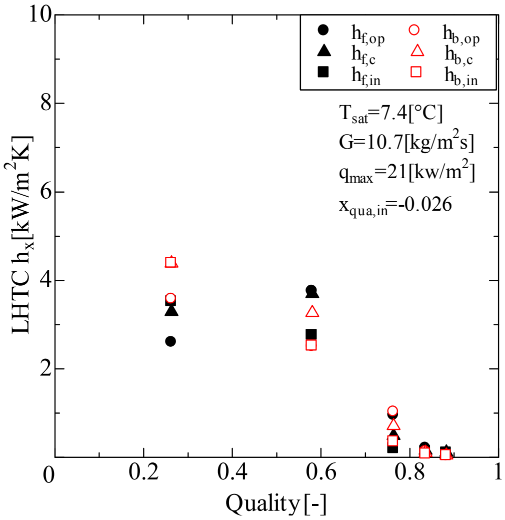

Figure 8: Local heat transfer coefficient of evaporation experiment (G = 10 kg/m^{2}s)

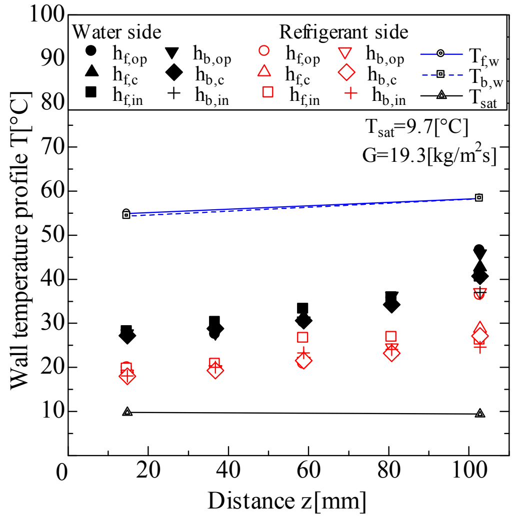

Figure 9: Temperature distribution of wall in evaporation experiment (G = 20 kg/m^{2}s)

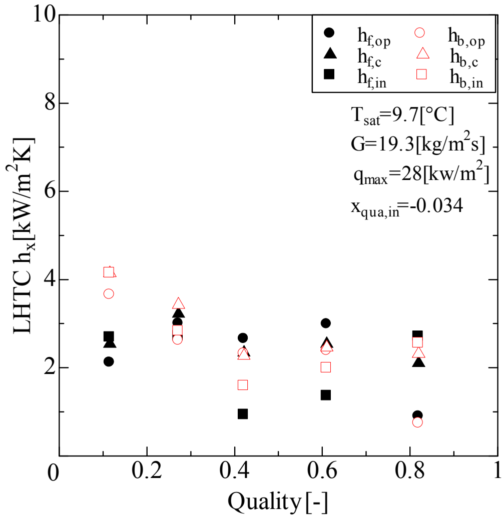

Figure 10: Local heat transfer coefficient of evaporation experiment (G = 20 kg/m^{2}s)

4. CONCLUSION

In order to obtain local heat transfer coefficient during condensation and evaporation in plate heat exchanger, a special test section has been produced where the channel is formed with two stainless steel plate having chevron grooves. Experiments on condensation and evaporation of R1234ze(E) have been carried out and the following results were obtained.

(1) From the measured wall temperatures at 60 points in the heat transfer wall, local heat transfer behavior is considered for condensation and evaporation experiments.
(2) In condensation experiment, notable temperature differences between inlet and opposite sides of the plate channel were identified. On the other hand, the temperature differences between front and back were small.
(3) Condensation heat transfer coefficient in low wetness region was two time higher than the Nusselt's equation for vertical plate. After that it decreases towards the Nusselt' equation and finally the measurement indicates lower value than the calculation.
(4) In evaporation experiment, the temperature differences between inlet and opposite were small except high quality region where dryout occurred.
(5) In both the condensation and evaporation, it is inferred that a maldistribution of refrigerant flow occurs and it affects on the heat transfer behavior.

REFERENCES

Asano, H., Takenaka, N, Wakabayashi, T. and Fujii T., 2007, Visualization and void fraction distribution of downward gas–liquid two-phase flow in a plate heat exchanger by neutron radiography, Nuclear Instruments and Methods in Physics Research Section A: Accelerators, Spectrometers, Detectors and Associated Equipment, 542(1-3): 154-160.

Arima, H., Mishima, F., Koyama, K., Fukunami, K. and Ikegami Y., 2012, Study on void fraction measurement of ammonia boiling heat transfer in plate evaporator, Proc. 49th NHTS, NHTS: A232, (in Japanese).

Kawazoe, A., Kariya K. and Miyara A., 2015, Measurements of local heat transfer coefficient during condensation and evaporation in a plate heat exchanger, Proc. the 24th IIR International Congress of Refrigeration (ICR2015): 847 (CDROM).

Longo, G.A., 2010, Heat transfer and pressure drop during HFC refrigerant saturated vapour condensation inside a brazed plate heat exchanger, Int. J. Heat and Mass Transfer, 53: 1079-1087.

Longo, G.A., Zilio, C., Righetti, G. and Brown, J.S., 2014. Condensation of the low GWP refrigerant HFO1234ze(E) inside a brazed plate heat exchanger, Int. J. Refrigeration 38: 250-259.

Longo. G.A., 2012, Vaporisation of the low GWP refrigerant HFO1234yf inside a brazed plate heat exchanger. Int. J. Refrigeration 35: 952-961.

Longo. G.A., 2012. Condensaion of the low GWP refrigerant HFO1234yf inside a brazed plate heat exchanger. Int. J. Refrigeration 36: 612-621

Eshima, Y., Mustaghfirin, M A. and Miyara, A., 2013, An experimental study of two-phase flow in plate heat exchangers, Proc. 2013 JSRAE Annual Conf., JSRAE: 331-334 (in Japanese).

Yan, Y-Y., Lio, H.C. and Lin, T.F., 1999, Condensation heat transfer and pressure drop of refrigerant R-134a in a plate heat exchanger, Int. J. Heat and Mass Transfer, 42: 993-1006.

Miyara, A., Onaka, Y. and Koyama, S., 2012, Ways of next generation refrigerants and heat pump/refrigeration systems, Int. J. Air-Conditioning and Refrigeration, 20(1): 1130002.

ACKNOWLEDGEMENT

This study was sponsored by the project on "The Development of Non-fluorinated Energy-saving Refrigeration and Air Conditioning Systems" of New Energy and Industrial Technology Development Organization (NEDO), Japan.